Available online at www.sciencedirect.com
ScienceDirect
Biochemical and Biophysical Research Communications 356 (2007) 85–90
BBRC
www.elsevier.com/locate/ybbrc

Inactivation of Mxi1 induces Il-8 secretion activation in polycystic kidney

Kyung Hyun Yoo [a,1], Young Hoon Sung [b,1], Moon Hee Yang [a,1], Jeong Ok Jeon [a], Yeon Joo Yook [a], Yu Mi Woo [a], Han-Woong Lee [b,*], Jong Hoon Park [a,*]

[a] *Department of Biological Science, Sookmyung Women's University, Seoul 140-742, Republic of Korea*
[b] *Department of Biochemistry, Yonsei University, Seoul 120-749, Republic of Korea*

Received 13 February 2007
Available online 28 February 2007

Abstract

The Mxi1 proteins are biochemical and biological antagonists of c-myc oncoprotein. It has been reported that the overexpression pattern of c-myc might be similar to a molecular feature of early and late stages of human autosomal dominant polycystic kidney disease. We identified the cyst phenotype in Mxi1-deficient mice aged 6–12 months using H&E staining. Some chemokines containing a protein domain similar to human IL-8, which is associated with the inflammatory response, were subsequently selected from the up-regulated genes. We confirmed the expression level of these chemokines and measured protein concentrations of IL-8 using ELISA in the Mxi1-knockdown cells. IL-8 was found to be significantly increased in Mxi1-knockdown cells. We found that p38 MAP kinase activation was involved in the signal transduction of the Mxi1-inactivated secretion of IL-8. Therefore, we could suggest that the inactivation of Mxi1 leads to the inflammatory response and has the potential to induce polycystic renal disease.

Keywords: Mxi1; IL-8; Polycystic kidney; Inflammatory response; p38

The Mxi1 gene is located at 10q24–q25. This region is known to be a cancer hotspot [1]. Deletions or rearrangements of the Mxi1 gene cause several kinds of cancer in humans. Deletion of the Mxi1 gene frequently results in events, such as tumors in humans; the loss of this gene has been detected in 9–62% of prostate tumors, 12–32% of renal cell carcinomas, 5–26% of meningiomas, 40% of endometrial cancers, 74–91% of small-cell lung cancers, and 13–93% of gliomas. Loss of the 10q sequence in human tumors may be associated with Mxi1 gene activity [2]. In addition, Mxi1 proteins have been suggested to be essential in controlling cellular growth and in inducing and maintaining the differentiated state. Consistent with these roles, Mxi1 may be a tumor-suppressor gene [3].

Autosomal dominant polycystic kidney disease (ADPKD) is one of the most common human monogenic diseases, with an incidence of 1:400 to 1:1000, and is a serious, life-threatening genetic disease in which extensive epithelial-lined cysts develop in the kidneys and, to a lesser extent, in other organs such as the liver, pancreas, and ovaries [4]. In a majority of cases (80–85%), the gene involved is PKD1, which is located on chromosome 16q13.3 and encodes polycystin-1, a large receptor-like integral membrane protein that contains several extracellular motifs indicative of cell–cell and cell–matrix interaction. In the remaining (10–15%) cases, the disease is milder and is caused by mutational changes in another gene, PKD2, which is located at chromosome 4q21–23 and encodes polycystin-2, a transmembrane protein that acts as a nonspecific calcium-permeable channel. Both polycystins function together in a nonredundant fashion, through a common pathway, and produce cellular responses that regulate proliferation, migration, differentiation, and kidney morphogenesis. Loss of function of either protein due to gene mutation results in the tubular cells reverting to a less

* Corresponding authors. Fax: +82 2 362 8096 (H.-W. Lee), +82 2 2077 7322 (J.H. Park).
E-mail addresses: hwl@yonsei.ac.kr (H.-W. Lee), parkjh@sookmyung.ac.kr (J.H. Park).
[1] These authors equally contributed to this work.

0006-291X/$ - see front matter © 2007 Elsevier Inc. All rights reserved.
doi:10.1016/j.bbrc.2007.02.103

differentiated state, which causes them to be more prone to proliferation [5–12].

Here, we used H&E staining to demonstrate that inactivation of Mxi1 leads to a cystic phenotype. We screened the gene expression pattern by microarray. Chemokines containing a protein domain, having the similarity to IL-8 that was related to the inflammatory response, were subsequently selected among the up-regulated genes. In addition, we found that p38 MAP kinase activation is involved in the signal transduction of the Mxi1-inactivated IL-8 secretion.

Materials and methods

Tissue sampling. Renal tissue was isolated from Mxi1-deficient mice aged 6–12 months and age-matched mice used as controls. For RT-PCR, kidney tissues were taken from sacrificed mice and immediately snap-frozen. For histological analysis, tissues were fixed in freshly prepared 4% paraformaldehyde in PBS, dehydrated with graded ethanol, cleared in xylene, and embedded in paraffin.

Histological analysis. Slides prepared with 10 μm sections were stained with hematoxylin and eosin. Sections were deparaffinized with Histo-clear II and rehydrated with graded ethanols. After slides had been rinsed for 10 min in 3′ distilled water, they were incubated with hematoxylin (LAB VISION, TA-125-MH) for 1 min 30 s. Slides were washed, and incubated with eosin (Sigma, E4382-25G) for 1 min. Finally, the tissue sections were dehydrated with graded ethanol solutions, and covered with glass coverslips.

Total RNA extraction and real-time RT-PCR. Total RNA was extracted by using an RNeasy Tissue Mini kit (Qiagen, No. 74104) according to the instructions of the manufacturer and treated with DNase at 37 °C for 40 min in order to protect against genomic DNA contamination. RNA was cleaned using an RNeasy kit (Qiagen, No. 74104). Total RNA synthesized cDNA using the QuatiTect® Reverse Transcription kit (Qiagen, No. 205311). The reaction of Q-PCR were determined using the real-time PCR SYBR green kit (Qiagen, No. 204143). The primers used was: 18s rRNA, sense 5′-GTAACCCGTTGCACCCCATT-3′, antisense 5′-CCATCCAATCGGT AGTAGCG-3′; CKL12 (chemokine ligand 12), sense 5′-GGGAACTTCA GGGGGAAATA-3′, antisense 5′-GGGAAGCTGTGATCTTCAGG-3′; CKL14 (chemokine ligand 14), sense 5′-GAAGGGGCCCAAGATC CGCTACAG-3′, antisense 5′-TGGACATGCTCTTGGTGGTGACGA-3′; CKL19 (chemokine ligand 19), sense 5′-GACCTTCCCAGCCCCAAC TCT-3′, antisense 5′-CACCCTGCAGCCATCTTCATTA-3′. The reaction was then performed in the Rotor-gene 3000® (Corbett Robotics, San Francisco, CA) according to the protocol of the manufacturer. Also, the primers used in Quantitative RT-PCR were: GAPDH, sense 5′-AACTTTG GCATTGTGGAAGG-3′, antisense 5′-ACACATTGGGGGTAGGAA CA-3′; CKL19, sense 5′-CAAGAACAAAGGCAACAGCA-3′, antisense 5′-CGGCTTTATTGGAAGCTCTG-3′; CKL12, sense 5′-GGGAAGC TGTGATCTTCAGG-3′, antisense 5′-GGGAACTTCAGGGGGAAAT A-3′, CKL14, sense 5′-GTCGGCTGCTTTGGTAGAAG-3′, antisense 5′-TATTCACTGAGGGGGAGTGC-3′; Irf1, sense 5′-AGGGCTTAGG AGGCAGAGTC-3′, antisense 5′-TCTAGGGCCAGTGCTATGCT-3′; H2-Eb1, sense 5′-CTGGAACACCACAACCTCCT-3′, antisense 5′-CTCT GAGGAACCGTCTCCAG-3′; H2-Q10, sense 5′-AGGCTGGTGCTG CAGAGTAT-3′, antisense 5′-AGTTCCATGTCCTGGGTCAG-3′; Krt2-5, sense 5′-TCAAGAAGCAGTGTGCCAAC-3′, antisense 5′-TCCAGC AGCTTCCTGTAGGT-3′; Krt1-19, sense 5′-CTCGGATTGAGGAG CTGAAC-3′, antisense 5′-TCACGCTCTGGATCTGTGAC-3′; Mtap7, sense 5′-CCACAGCCTTCTGAGACTCC-3′, antisense 5′-AGCCAGGG CTACACAGAGAA-3′; Lamb3, sense 5′-GGCTCCCTAATGTGGAC TCA-3′, antisense 5′-TGCATTGTGTCCTGAGCTTC-3′; Dpt, sense 5′-GGATCGTGAGTGGCAATTTT-3′, antisense 5′-CGAATTCGCAG TCGTAGTCA-3′; Sprr2a, sense 5′-TCCTGTCATGTGCTTTGAGC-3′, antisense 5′-CCTGTTGGGTGGTCACTTCT-3′; Mxi1, sense 5′-GC AACACCAGCACTGCCAAC-3′, antisense 5′-AGGAGACTGCAT GAACC-3′.

Microarray. We utilized the UniSet Mouse Expression Bioarray (Code-Link bio-array) containing 20,000 gene probes. This array contains a broad range of genes derived from publicly available, well-annotated mRNA sequences. The CodeLink array is unique in that it is capable of detecting minimal differences in gene expression, as low as 1.3-fold with 95% confidence. Ten micrograms of total RNA was amplified and labeled cRNA was produced using the kit available from Amersham and designed for use with the CodeLink® arrays. Biotin-labeled cRNA was hybridized to the array overnight in a shaking incubator at 37 °C and excess target sequence was washed away using a series of SSC washes. The array was stained by treatment with streptavidin-Alexaflour 647 (Molecular Probes), the excess was washed away, and the array was scanned at an excitation wavelength of 632 nm using an Axon Instruments GenePix scanner. The resulting image was quantified and the intensity of each spot was divided by the median spot intensity to provide a scaled and comparable number across multiple arrays. Bacterial spots provided both positive and negative controls.

Cell culture and siRNA. HEK293T cell lines were cultured in Dulbecco's modified Eagle's medium (JBI) supplemented with 10% heat-inactivated (56 °C, 30 min) Fetal Bovine Serum (JBI), 100 U/ml penicillin and 100 μg/ml streptomycin in humidified air (CO_2, 5%) at 37 °C. After 48 h, cells were transfected using Lipofectamine 2000 reagent (Invitrogen) and 25 nM of siRNA directed against Mxi1. The Mxi1 target sequence used was: sense 5′-GAAUACGAAUGGACAGCAUTT-3′, antisense 5′-AUGCUGUCCAUUCGUAUUCTT-3′. After 48 h transfection, the efficiency of the knockdown was analyzed at the mRNA level using quantitative RT-PCR.

Enzyme linked-immuno sorbent assay (ELISA). Cells were cultured in 6-well tissue culture plates until reaching 70–80% confluence. The medium was harvested at 48 h after treatment. IL-8 was determined with an enzyme-linked immunosorbent assay (ELISA), using commercially available kits (Biosource, KHC0081).

Western blot analysis. Cell extracts from untreated and treated Mxi1 anti-sense, PD98059, and SB203589 were quantitated using a protein assay kit (Intron, 17081). Equal amounts of proteins (30 μg/lane) were separated on SDS–PAGE and electrotransferred to 0.45 μm PVDF membranes. The membranes were blocked with 5% skimmed milk solution and probed with anti-ERK (Cell signaling, 9102, 1:100), anti-pERK (Cell signaling, 4377, 1:100), anti-p38 (Cell signaling, 9212, 1:100), and anti-pp38 (Cell signaling, 9211, 1:50).

Results

Phenotype of the Mxi1-deficient mouse

To confirm the phenotype caused by the inactivation of the Mxi1 gene, histological examinations were conducted in the kidneys of the Mxi1-deficient mice aged 6–12 months. On histopathologic examination, multiple tubular cysts were observed in the renal tissue of Mxi1-deficient mouse founders aged 6–12 months. It is reported that dilation of the Bowman's space appeared in the Mxi1-deficient mouse aged 7 months or more [3]. Here, we found new phenotypes as well as changes of glomeruli in these mice. Many typical enlarged cysts were observed in the cortex region of the kidney and they were composed of a single layer of slightly flattened cells. We called these growths cysts when their size was larger than 150 μm because this is three times the normal tubule size. These alterations appear similar to those described in human ADPKD. In ADPKD, cyst formation was occurred following increased

proliferation of tubular epithelial cells. In Fig. 1A and B, we are able to observe cysts lined by overproliferation of tubular epithelial cells, which indicated early and intermediate stages of cystogenesis. We also found that tubular epithelial cells changed shape, from cuboidal to flat, and found that the cyst lining appeared to be composed of a single layer (Fig. 1C–E), which represented the later stages of cystogenesis. We assessed the shape of the Bowman's capsules in an identical study of dilated glomeruli that was conducted previously (Fig. 1F). Inflammatory cells were observed in the vicinity of the cysts (Fig. 1G) and we also found abnormal tubules similar to those seen in hyperplasia and neoplastic growth (Fig. 1A, C, and H). From these results, we suggest that inactivation of Mxi1 is induced abnormally in the kidney.

Gene expression analysis

In ADPKD, the cyst formation mechanism was not yet clear. In order to understand the mechanism of cyst formation related with ADPKD in kidney, we performed microarray using Mxi1-deficient mice. We compared the pattern of gene expression between the Mxi1-deficient mouse kidney and that of wild-type mouse using microarray in a 20 K mouse oligonucleotide (CodeLink bioarray) chip for 20,000 genes. All the statistical methods used for the microarray data analysis were performed using the R package (Bioconductor). As a result, we found 49 genes up-regulated and 96 genes down-regulated in the Mxi1-deficient mouse. Table 1 shows a list of genes that were which related with the immune response and inflammation among the up-regulated genes in the Mxi1-deficient mouse. This list included several chemokines, Histocompatibility class I and Histocompatibility class II. In addition, chemokines (chemokine Ligand 12, chemokine ligand 14 and chemokine ligand 19) containing a protein domain similar to human IL-8, is associated with the inflammatory response in polycystic kidney disease, were included in this list. Table 2 shows a list of genes associated with cell structure among the down-regulated genes in the Mxi1-deficient mouse. This gene list included keratin complex, laminin beta 3, cathepsin E, and microtule-associated protein 7.

To verify the results obtained by microarray analysis, differentially expressed transcripts representing up-regulated or down-regulated genes were analyzed for differential expression by semi-quantitative RT-PCR (Fig. 2A). In our results, the expression of genes corresponded with microarray data. We selected chemokine ligand 12, chemokine ligand 14, and chemokine Ligand 19 among the up-regulated genes because that it is well-known that IL-8 serves as an autocrine and paracrine factor to direct errant growth of ADPKD [13]. We confirmed the expression levels of these genes using real-time RT-PCR. As a result, these genes were increased in Mxi1-deficient mice (Fig. 2B). The CKL12 gene was increased 4.6 fold (4.63 ± 0.53033), the CKL14 gene was increased 1.6 fold (1.66 ± 0.23335) and the CKL19 gene was increased 4.3 fold (4.30 ± 0.53033) in 1-year-old Mxi1-deficient mice aged compared to the control mice. These results indicated that microarray data showed reliable results and inactivation of Mxi1 leads to the the increase several chemokines that are similar to the human IL-8 domain.

Inactivation of Mxi1 induces IL-8 secretion

To investigate whether inactivation of Mxi1 induces secretion of IL-8, we performed siRNA-mediated knockdown of Mxi1 in the HEK293T cell line. As expected, knockdown of Mxi1 decreased mRNA expression as measured by semi-quantitative RT-PCR. We measured protein

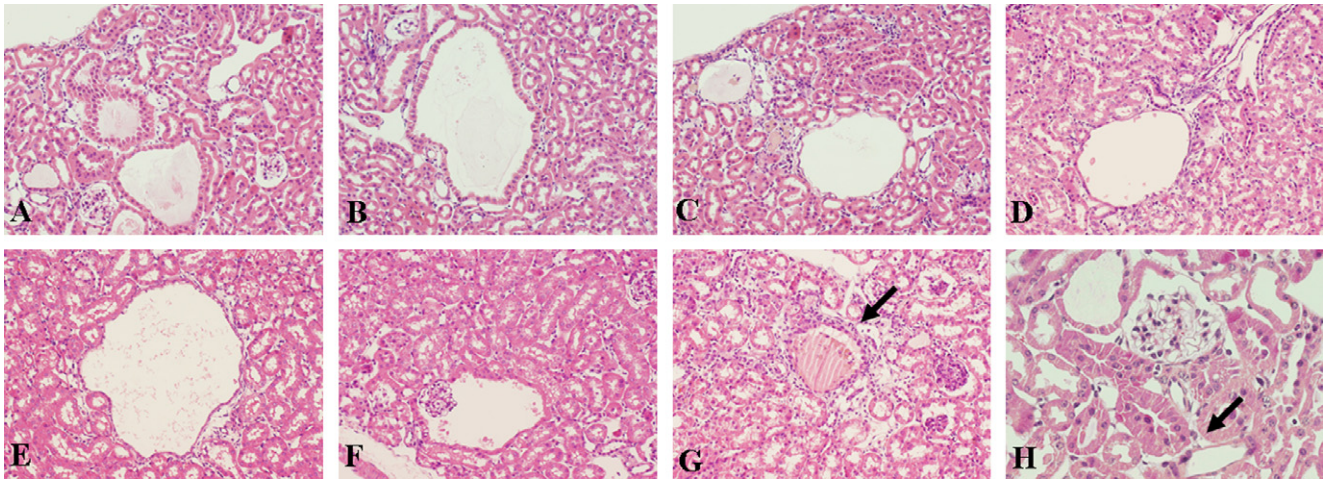

Fig. 1. Hematoxylin & Eosin-stained kidney from Mxi1-deficient mice aged 6–12 months. The typical enlarged cysts, of which lining epithelia were composed of a single layer of slightly flattened cells, were larger than 150 μm in size (A–E). The shapes of the Bowman's capsules dilated glomeruli (F). Inflammatory cells around cysts (arrow) (G). Hyperplasia cells around cysts (arrow) (H). Overproliferative cells at the early and intermediated stage of cystogenesis (A,B). Tubular epithelial cells changed shape from cuboidal to flat and the cyst lining showed a single layer at late stage of cystogenesis (C–E). Mxi1-deficient mouse aged 6 months (A–C), 9 months (D), and 12 months (E–H), Original magnification: 200× (A–G), 400× (H).

Table 1
Up-regulated genes in the Mxi1-deficient mouse kidney

NCBI_No.	Gene description	Fold
NM_011888.2	Chemokine (C–C motif) ligand 19	3.74
NM_010386.2	Histocompatibility 2, class II, locus DMa	3.60
NM_010382.1	Histocompatibility 2, class II antigen E beta	3.18
NM_010391.1	Histocompatibility 2, Q region locus 10	2.73
NM_008390.1	Interferon regulatory factor 1	2.61
NM_008326.1	Interferon inducible protein 1	2.43
NM_011331.1	Chemokine (C–C motif) ligand 12	2.35
NM_013517.1	Fc receptor, IgE, low affinity II, alpha polypeptide	2.18
NM_019568.1	Chemokine (C–X–C motif) ligand 14	2.09

Table 2
Down-regulated genes in the Mxi1-deficient mouse kidney

NCBI_No.	Gene description	Fold
NM_011468.2	Small proline-rich protein 2B	0.21
NM_009264.1	Small proline-rich protein 1A	0.21
NM_027011.1	Keratin complex 2, basic, gene 5	0.21
AK003138.1	Adipocyte, C1Q and collagen domain containing	0.29
NM_008471.1	keratin complex 1, acidic, gene 19 (Krt1–19)	0.30
NM_008484.1	Laminin beta 3	0.35
NM_007799.2	Cathepsin E	0.37
NM_009964.1	Crystallin, alpha B	0.41
NM_010664.1	Keratin complex 1, acidic, gene 18	0.44
NM_008635.1	Microtubule-associated protein 7	0.48
NM_019759.1	Dermatopontin	0.49

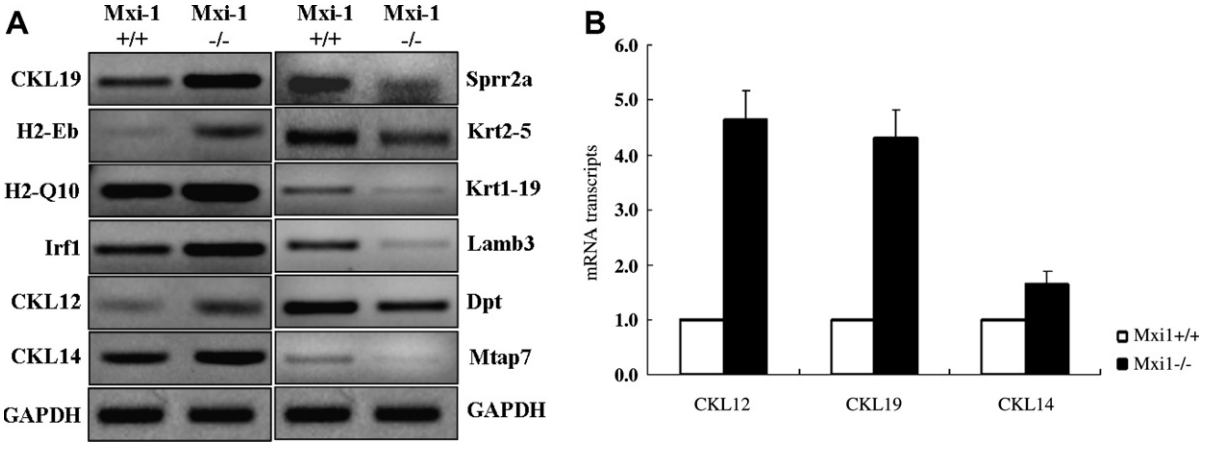

Fig. 2. The verification of candidate genes obtained by microarray. The expression of up-regulated and down-regulated genes by semi-quantitative RT-PCR (A). Up-regulated genes were increased in the Mxi1-deficient mouse. Down-regulated genes were decreased compare with wild type mouse. The expression of CKL12, CKL14, and CKL19 mRNA by real-time RT-PCR (B). The CKL12 gene was increased 4.6 times (4.63 ± 0.53033), the CKL14 gene was increased 1.6 times (1.66 ± 0.23335) and the CKL19 gene was increased 4.3 times (4.30 ± 0.53033) in the Mxi1-deficient mouse aged 1 year compared to the control mice.

concentrations of IL-8 through ELISA in the culture medium of Mxi1 knockdown cells. IL-8 was found to be significantly increased in Mxi1 knockdown cells when compared with the control group (Figs. 3 and 4). From these results, we confirmed inactivation of Mxi1 induced secretion of IL-8. To determine the functional roles of extracellular signal-regulated kinase (ERK) and the p38 MAP kinase pathway during Mxi1-inactivated IL-8 secretion, we used the ERK specific inhibitor, PD98059, to prevent ERK activation, and used SB203589 for p38 inhibition. Fig. 3 shows whether ERK was related to Mxi1-inactivated IL-8 secretion. We measured of IL-8 concentration in cells which untreated and treated with Mxi1 anti-sense and PD98059. The results measure of IL-8 concentration, IL-8 concentrations were increased 2.5 times in group treated with Mxi1 anti-sense than untreated cells. In addition, when treated with Mxi1 anti-sense and PD98059 at final concentrations of 12.5, 25, and 50 μM, IL-8 concentrations remained quite high. In order to confirm Mxi1 decreased mRNA expression in the Mxi1 knock-down cells, we performed quantita-

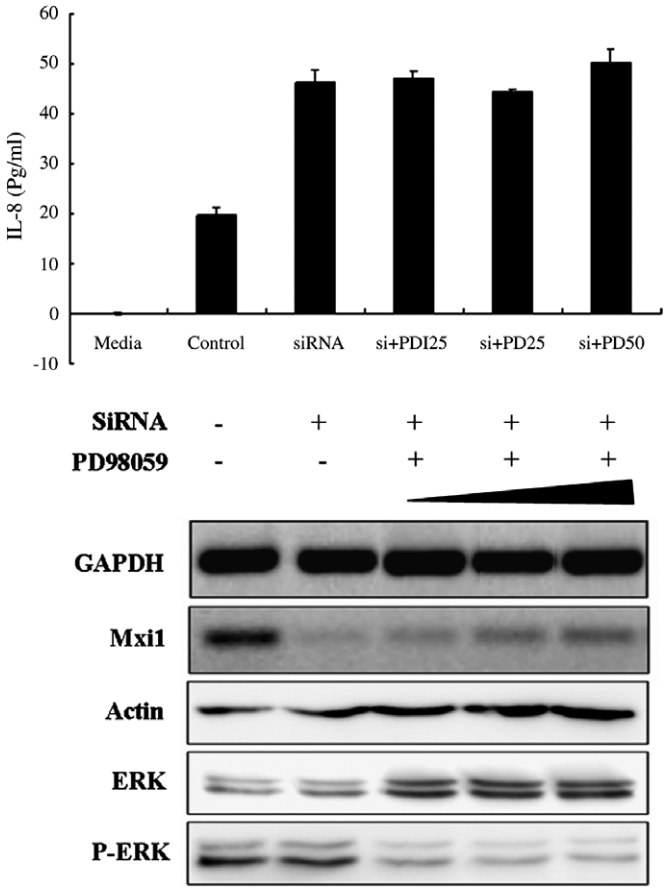

Fig. 3. Inhibitory effects of the Mxi1 antisense and ERK-specific inhibitor (PD98059) in HEK293T cells. Measurement of IL-8 concentration using ELISA. IL-8 concentration was found to be significantly increased in Mxi1 knock-down cells (46.0494 ± 2.6390 pg/ml) when compared with the control group (19.784 ± 1.3640 pg/ml). Groups treated with PD98059 at final concentrations of 12.5 μM (46.9445 ± 1.5885 pg/ml), 25 μM (44.4753 ± 0.3252 pg/ml), and 50 μM (50.4321 ± 2.6369 pg/ml) were also significantly increased when compared with the control group.

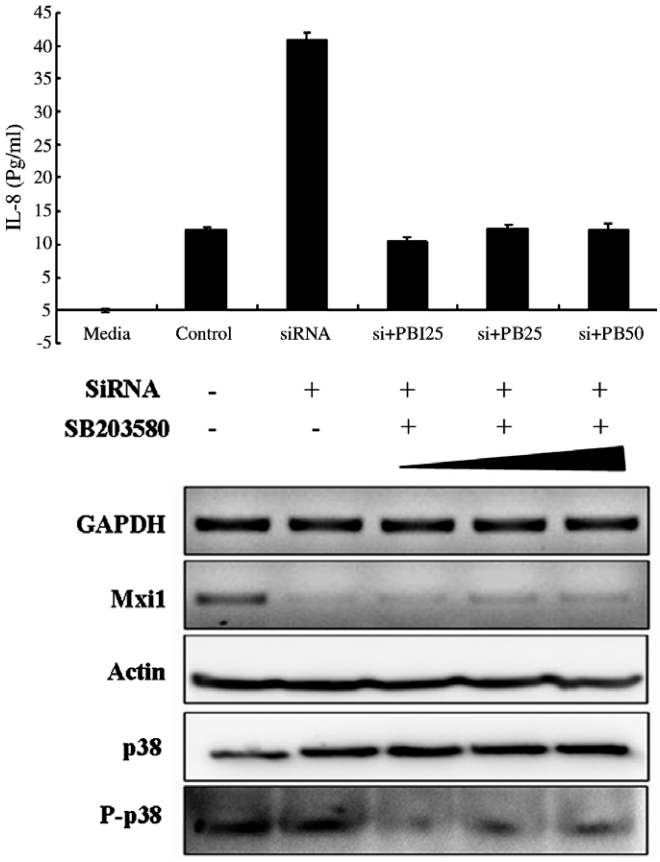

Fig. 4. Inhibitory effects of the Mxi1 antisense and p38-specific inhibitor (SB203589) in HEK293T cells. Measurement of IL-8 concentration using ELISA. IL-8 concentration was found to be significantly increased in Mxi1 knock-down cells (46.8334 ± 1.1201 pg/ml) when compared with the control group (12.2531 ± 0.2673 pg/ml). Groups treated with PD98059 at final concentrations of 12.5 μM (10.3704 ± 0.6165 pg/ml), 25 μM (12.5 ± 0.2976 pg/ml), and 50 μM (12.1297 ± 0.9637 pg/ml) were significantly decreased.

tive RT-PCR. To confirm the inhibitory effect of PD98059, we performed immunoblotting using cell lysates from cells that were untreated or treated with Mxi1 anti-sense and PD98059. From these results, ERK activation did not have a part in Mxi1-inactivated IL-8 secretion. We performed the same experiments in order to determine the inhibitory effect of SB203589, a p38-specific inhibitor (Fig. 4). In our results, we confirmed a decrease of Mxi1 mRNA expression in treated with Mxi1 anti-sense and a decrease of p38 activation in groups treated with SB203589. In groups treated with Mxi1 anti-sense and SB203589 at final concentrations of 12.5, 25, and 50 μM, IL-8 protein concentrations were significantly decreased compared with cells treated with only Mxi1 anti-sense. These results suggest that p38 MAP kinase is involved in the signal transduction of the Mxi1-inactivated IL-8 secretion.

Discussion

Renal kidney disease is a major cause of end-stage renal failure. Several genes have been found to be involved in these disorders. However, the pathway related to cyst formation remains unclear. Mxi1 plays a crucial role in the maintenance of normal cell growth and differentiation. Inactivation of Mxi1 leads to cystic renal diseases such as ADPKD. Here we show that mice lacking Mxi1 suffer from severe cystic kidney disease.

We found abnormal phenotypes in the Mxi1-deficient mouse using H&E staining. The typical enlarged cysts, of which lining epithelia were composed of a single layer of slightly flattened cells, were larger than 150 μm in a size. We also determined the shapes of the Bowman's capsules in dilated glomeruli, and noted hyperplasia and inflammatory cells around cysts. Our lab already checked the change of expression genes related with renal disease in the Mxi1-deficient mouse. Inactivation of Mxi1 leads to increases in c-myc, an antagonist of the Mxi1. This plays an important part in cyst formation in other renal diseases as well as ADPKD. In one-year-old Mxi1-deficient mice, we confirmed that c-myc expression was increased to twice that of control mice. Moreover, we identified that the expressions of PKD1 and PKD2 were increased in the Mxi1-deficient mice. Our results suggest that changes in these genes

will play an important part in cyst formation. It has already been reported that the expression of c-myc was increased in the PKD1 transgenic mouse model [14]. We expect that the change of expression these genes affects abnormal phenotype which is cyst formation, inflammatory cells, and hyperplasia in the Mxi1-deficient mouse.

To investigate the mechanism of cystogenesis, we used microarray analysis to search for genes that are differentially expressed between Mxi1-deficient and wild-type mice. In this investigation, we found up-regulated genes involved with several chemokines connected with the inflammatory and immune systems. Chemokines (CKL12, CKL14, and CKL19) containing a protein domain similar to IL-8, which is related to the inflammatory response, were subsequently selected from the up-regulated genes. It is well-known that IL-8 serves as an autocrine and paracrine factor to direct aberrant growth of ADPKD liver cyst epithelia [13,15].

To identify whether inactivation of Mxi1 induces the secretion of IL-8, we performed siRNA-mediated knockdown of the Mxi1 in the HEK293T cell line. IL-8 was found to be significantly increased in Mxi1 knockdown cells when compared with the control group. This result suggests that the inactivation of Mxi1, which leads to increased IL-8 secretion, has an effect on cyst growth and enlargement in ADPKD. In addition, we investigated the involvement of extracellular signal-regulated kinase (ERK) and of p38 MAP kinase in the signal transduction of Mxi1-inactivated IL-8 secretion, and found that the presence of a specific inhibitor of p38 MAP kinase, blocked Mxi1-inactivated secretion of IL-8. These results demonstrate that the activation of p38 MAP kinase is involved in the signal transduction observed in the Mxi1-inactivated secretion of IL-8. It is known that a variety of extracellular stimuli such as growth factors, cytokines, and cellular stress can be activated by the p38 MAPK signaling pathway. Moreover, this leads to the regulation of inflammatory cytokine production e.g., IL-1β, TNF-α, and IL-6, in addition to the regulation of the differentiation and proliferation of cells in the immune system. Thus, it is widely accepted that p38 MAP kinase plays an important role in the regulation of the inflammatory response [16].

Therefore, the findings of this study may suggest that the inactivation of Mxi1 leads to an inflammatory response through p38 MAP kinase and has the potential to induce polycystic renal disease.

Acknowledgments

This work was supported by the Korea Science and Engineering Foundation (KOSEF) through the National Research Lab. Program funded by the Ministry of Science and Technology (M10500000101-06J0000-10110), KOSEF grant funded by the Korea government (MOST) (ROI-2004-000-10182-0), Grants from 21C Frontier FHGP (FG05-22-02) and the BRC Frontier (M103KV010018-05K2201-01830). We are grateful to Dr. J.Y. Noh at Sookmyng Women's University for discussions.

References

[1] E.V. Prochownik, L. Eagle Grove, D. Deubler, X.L. Zhu, R.A. Stephenson, L.R. Rohr, X. Yin, A.R. Brothman, Commonly occurring loss and mutation of the MXI1 gene in prostate cancer, Genes Chromosomes Cancer 22 (1998) 295–304.

[2] D.Y. Wang, Y.Y. Xiang, X.J. Li, M. Hashimoto, M. Tanaka, H. Sugimura, Mxi1 is a potential cellular target of carcinogens and frequently mutated in experimental rat tumors and tumor cell lines, Pathol. Int. 50 (2000) 373–383.

[3] N. Schreiber-Agus, Y. Meng, T. Hoang, H. Hou Jr., K. Chen, R. Greenberg, C. Cordon-Cardo, H.W. Lee, R.A. DePinho, Role of Mxi1 in ageing organ systems and the regulation of normal and neoplastic growth, Nature 4 (1998) 483–487.

[4] A.C. Ong, P.C. Harris, Molecular pathogenesis of ADPKD: the polycystin complex gets complex, Kidney Int. 67 (2005) 1234–1247.

[5] S.T. Reeders, T. keith, P. Green, G.G. Germino, N.J. Barton, O.J. Lehmann, V.A. Brown, P. Phipps, J. Morgan, J.C. Bear, Regional localization of the autosomal dominant polycystic kidney disease locus, Genomics 3 (1988) 150–155.

[6] W.J. Kimberling, S. Kumar, P.A. Gabow, J.B. Kenyon, C.J. Connolly, S. Somlo, Autosomal dominant polycystic kidney disease: localization of the second gene to chromosome 4q13–q23, Genomics 18 (1993) 467–472.

[7] D. Ravine, R.G. Walker, R.N. Gibson, S.M. Forrest, R.I. Richards, K. Friend, L.J. Sheffield, P. Kincaid-Smith, D.M. Danks, Phenotype and genotype heterogeneity in autosomal dominant polycystic kidney disease, Lancet 340 (1992) 1330–1333.

[8] J. Hughes, C.J. Ward, B. Peral, R. Aspinwall, K. Clark, J.L. San Millan, V. Gamble, P.C. Harris, The polycystic kidney disease 1 (PKD1) gene encodes a novel protein with multiple cell recognition domains, Nat Genet. 10 (1995) 151–160.

[9] T.C. Burn, T.D. Connors, W.R. Dackowsik, L.R. Petry, T.J. Van Raay, J.M. Millholland, M. Venet, G. Miller, R.M. Hakim, G.M. Landes, et al., Analysis of the genomic sequence for the autosomal dominant polycystic kidney disease (PKD1) gene predicts the presence of a leucine-rich repeat. The American PKD1 Consortium (APKD1 Consortium), Hum. Mol. Genet. 4 (1995) 575–582.

[10] P.C. Harris, C.J. Ward, B. Peral, J. Hughes, Polycystic kidney disease. 1: Identification and analysis of the primary defect, J Am Soc Nephrol. 6 (1995) 1125–1133.

[11] T. Mochizuki, G. Wu, T. Hayashi, S.L. Xenophontos, B. Veldhuisen, J.J. Saris, D.M. Reynolds, Y. Cai, P.A. Gabow, A. Pierides, W.J. Kimberling, M.H. Breuning, C.C. Deltas, D.J.M. Peters, S. Somlo, PKD2, a gene for polycystic kidney disease that encodes an integral membrane protein, Science 272 (1996) 1339–1342.

[12] F. Quian, F.J. Germino, Y. Cai, X. Zhang, S. Somlo, C.G. Germino, PKD1 interacts with PKD2 through a probable coiled-coil domain, Natrue Genet. 16 (1997) 179–183.

[13] M.T. Nichols, E. Gidey, T. Matzakos, R. Dahl, G. Stiegmann, R.J. Shah, J.J. Grantham, J.G. Fitz, R.B. Doctor, Secretion of cytokines and growth factors into autosomal dominant polycystic kidney disease liver cyst fluid, Hepatology 40 (2004) 836–846.

[14] C. Thivierge, A. Kurbegovic, M. Couillard, R. Guillaume, O. Cote, M. Trudel, Overexpression of PKD1 causes polycystic kidney disease, Mol. Cell Biol. 26 (2006) 1538–1548.

[15] J.J. Grantham, G.F. Schreiner, L. Rome, L. Grenz, A. Joly, Evidence for inflammatory and secretagogue lipids in cyst fluids from patients with autosomal dominant polycystic kidney disease, Proc. Assoc. Am. Phys. 109 (1997) 397–408.

[16] K. Ono, J. Han, The p38 signal transduction pathway: activation and function, cell signal, Cell signal. 12 (2000) 1–3.